14 Aerosols

An aerosol is a suspension of small liquid droplets or solid particles in air or gas. The dispersion includes smoke, dust, fog, etc. and has enormous practical importance. Gas as a dispersion medium is different from liquid in two ways:

(1) The mean free path of the gas molecules can be comparable to the separation between particles (droplets), so that even local thermal equilibrium is not easily established in time when local disturbance, such as heat generation by condensation, occurs. Even when the medium can be considered to be continuous, its viscosity is orders of magnitude lower than that of liquids.
(2) The stability of an aerosol cannot be so readily modified by additions to the dispersion medium as in the flocculation of hydrosols by electrolyte or their stabilization by linear macromolecules such as steric effects. In some ways, aerosols are simpler than sols in condensed media.

Recently, a bioaerosol has drawn a wide attention (Lighthart and Mohr, 1994). It is defined as an aerosol whose components contain, or have attached to them, one or more microorganisms. Thus, it contains viruses, bacteria, fungi, protozoa, or algae, that are usually alive. Bioaerosols may be relatively solid particles or liquid particles and range from a single microorganism to large particles, which may change in size by condensation or evaporation. Many of the physical and chemical processes that describe aerosols also apply to bioaerosols.

14.1 Formation of Aerosols

Aerosols may be formed by either dispersion or condensation processes. Clusters vapor molecules act as centers of condensation for other vapor molecules and grow rapidly to a size of about 0.1 μm. Thermal, or Brownian, coagulation then becomes the predominant mechanism for further growth (Walter, 1973).

There are various other mechanisms for a new particle to appear in the atmosphere. Existing particles at a surface can become detached by wind stresses and other natural or artificial mechanical stresses. Fragments can become detached from solid or liquid surfaces because of abrasion, cracking, weathering, breaking

waves, bursting bubbles and so on. Grinding processes experience great difficulty in producing particles much below 1 μm. The presence of very small particles (< 1 μm) in an aerosol produced by pulverization is more likely to have resulted from evaporation and recondensation than direct fragmentation from the bulk.

Atomizers, sprays, and other devices are commonly used for a variety of purposes. The principle of operation is to draw liquid into threads or sheets, usually under the shearing action of an air stream. The shearing action develops surface waves whose frequency depends on the liquid's surface tension, the velocity of flow and the dimension of the orifice. At high enough velocity, the frequency can be imaginary and the waves become unstable, breaking the threads or sheets into fragments or drops, the size of which is determined by the thickness of the thread or film. During such atomization processes a considerable amount of work must be done against viscous forces and adhesive energy of separating the liquid.

Consider a medium in which drops are formed at the tip of a capillary. If a high potential is applied between the capillary and the medium, the drops formed carry electric charges, like with an electrocapillarometer (see Sec. 10.2.4). Assume that the surface charge can not be easily discharged. The maximum charge which can be carried by a spherical drop of radius a without rupture is $8\pi(a^3\varepsilon_0\varepsilon\gamma)$, where ε is the dielectric constant of the medium and γ is the interfacial tension. If the amount of charge on a drop is larger than the maximum at the time of forming, each drop is observed under high-speed photography to split into many hair-like jets. This observation suggests that the breaking-up mechanism may also include unstable surface waves.

A much more important mechanism is the bursting of bubbles at a liquid surface, including the ocean surface. The mechanism involved is now fairly well understood (Woodcock et al., 1953; Blanchard, 1967). Woodcock et al. (1953) measured the size of sea-salt particles produced at the ocean surface to be in the range > 1 μm.

To produce aerosols of controllable size and near monodispersity (the standard deviation $\sigma < 0.1$), the condensation may be performed on preformed nuclei of the vapor of high-boiling liquids in a stream of inert carrier gas, N_2 or He (see Sec. 7.2). Nuclei are formed by condensing the vapor of some solid such as NaCl or AgCl. Their size critically depends on the furnace temperature. AgCl nuclei have a modal radius of 1.3 nm at 590°C. It is increased to 25 nm at 605°C. The liquid to be used for the condensation is vaporized in a boiler through which carrier gas is bubbled.

14.1.1 Homogeneous Nucleation of Vapor and Nucleation by Ions

Homogeneous nucleation process has been discussed in Chapt. 3. The nucleation of vapor by ions occurs at lower supersaturation than does homogeneous nucleation. An interesting observation is that for some vapors negative ions are more effective, for others positive, and some vapors show no difference. It implies that

the free energy ΔG of formation of the critical nucleus must include the sign of the charge of ions. The classical expression for this term is proportional to the square of the charge, not predicting this observation correctly.

14.1.2 Particle Growth Rate by Condensation

The particle growth must involve the rate of heat transport as well as mass transport. In practical cases, the gas is not stagnant and temperature does not remain constant with temperature gradient. Thus, the discussion on the growth rate in Chapts. 3, 7, and 11 in the continuum regime is not applicable for aerosols, unless the gas is dense.

Growth and evaporation of liquid droplets are determined by the nonstationary fluxes of vapor and heat to the droplets. These fluxes can be obtained by solving the stationary equations for diffusion and heat conduction around a spherical droplet, assuming stationary transport of mass and energy controlled by diffusion. The applicability of the solution is then restricted to spheres whose radii are large compared to the mean free path of the surrounding gas (continuum regime).

In the case of a droplet whose radius is much smaller than the mean free path of the surrounding gas (free molecule regime), the diffusion theory predicts mass fluxes at the droplet surface that are much higher than the rate of evaporation. Then, the vapor at the droplet surface cannot be kept saturated and the equilibrium is destroyed. Accordingly, the transport is under kinetic control and the stationary fluxes of mass and energy can be calculated by kinetic theory. If the droplet size is comparable to the gas mean free path (transition regime), the transport of mass and energy is partly under diffusion control and partly under kinetic control. At the surface a jump of temperature and vapor concentration occurs (Langmuir, 1915). There are various attempts to solve the transitional mass flux (Wagner, 1982). The numerical calculation for water vapor in air shows that the droplet temperature T_a remains nearly constant during the growth, but the bulk temperature approaches a limiting value as the bulk saturation ratio S_∞ gets closer to unity. Substantial temperature gradients only exist over the distance of 10 μm in the vicinity of the droplets, where there are mutual interactions of mass and heat flux. Fig. 14.1 shows a comparison between the computed and experimental results for the growth curves. It was found that an approximation that the temperature was nearly uniform did not work well for high supersaturation and high temperature gradient. Corrections for transitional transport and consideration on heat flux are required.

The above description on particle behavior in gases infers that it depends on the Knudsen number defined by

$$Kn = \frac{\text{Mean free path } \lambda \text{ of gas molecules}}{\text{Drop radius } a} \tag{14.1}$$

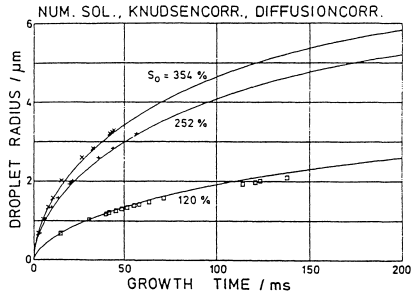

Fig. 14.1 Theoretical growth curves for water vapor in air at initial bulk saturation ratio $S_0 = 1.2$, 2.52, and 3.54, respectively. The symbols (□, +, and ×) are experimental data (Wagner and Pohl, 1978, 1979) for the respective ratio S_0. Droplet concentration is $4.6 \cdot 10^3$ cm^{-3} (Wagner, 1982, with permission from Springer-Verlag).

$$\lambda = \frac{3\eta_g}{2\rho_g}\left(\frac{\pi m_g}{2k_B T}\right)^{1/2} \tag{14.2}$$

where m_g is the mass of the gas molecule, η_g is the gas viscosity, and ρ_g is its density (Reichl, 1980).

In the binary mixture of vapor and gas, the mean free paths, λ_v and λ_g, of vapor and gas are, in general, different (Jeans, 1954). For low vapor concentration,

$$\lambda_v \approx \frac{m_g}{\sqrt{\frac{1+m_v}{m_g}}\rho_g \pi \sigma_{vg}}, \quad \lambda_g \approx \frac{m_g}{\sqrt{2}\rho_g \pi \sigma_g^2} \tag{14.3}$$

where m_v is the mass of the vapor molecule and σ_{vg} and σ_g are the collision cross-sections between vapor-gas and between gas-gas molecules, respectively. In the transition regime, the mass flux and heat transport depend on the Knudsen numbers:

$$Kn_M = \lambda_v / a \quad \text{and} \quad Kn_T = \lambda_g / a \tag{14.4}$$

respectively (Wagner, 1982). The heat flux seems not to have been successfully incorporated into the growth rate. The detailed behavior relative to the particle size is discussed by Hidy and Brock (1970). We consider the particle growth only intuitively as follows.

In a limiting case of the range of $Kn < 0.01$, the gas may be considered to be continuous and the diffusion coefficient of vapor in the gas can be introduced to express the flux of vapor. Then, the growth rate of a particle by condensation can be found by the diffusion equation, Eq. 7.15. From Eq. 7.17, the diffusion controlled growth rate is given by

$$\left(\frac{dm}{dt}\right)_D = 4\pi a D(c_\infty - c_a) \tag{14.5}$$

where D is the diffusion coefficient, a is the particle radius, and c_∞ and c_a are the vapor density at the bulk and the surface, respectively. If c_a is higher than the sat-

uration vapor pressure, the condensation may occur. Otherwise, evaporation will follow.

On the other end of the limiting case, $Kn \to \infty$, the transport of vapor is under kinetic control. From kinetic theory (Eq. 3.10), the number of vapor molecules which strike the particle surface per unit time is

$$\frac{1}{4} n \langle v \rangle \cdot 4\pi a^2 \tag{14.6}$$

where $\langle v \rangle$ is the mean speed of the vapor molecules and n is the number density of vapor molecules. Of these molecules a fraction α condenses and $1-\alpha$ is redispersed. Assuming that the vapor at the particle surface is almost saturated, the growth rate under the kinetic model is given by

$$\left(\frac{\mathrm{d}m}{\mathrm{d}t}\right)_k = \pi a^2 \alpha \langle v \rangle (c_\infty - c_a) \tag{14.7}$$

In the transition regime, it is supposed that at a distance δ from the surface of a droplet, which is small enough for diffusion control to fail to be applicable, the vapor concentration is denoted by c_δ. The kinetic control prevails up from the surface of the droplet to a radius $a+\delta$. Beyond this distance diffusion predominates. Since $\mathrm{d}m/\mathrm{d}t$ must be the same across each zone, we have

$$\mathrm{d}m/\mathrm{d}t = 4\pi(a+\delta)D(c_\infty - c_\delta) = \pi a^2 \langle v \rangle \alpha (c_\delta - c_a) \tag{14.8}$$

By eliminating c_δ, we obtain

$$\frac{\mathrm{d}m}{\mathrm{d}t} = \frac{(\mathrm{d}m/\mathrm{d}t)_D}{4D/a\langle v \rangle \alpha + a/(a+\delta)} \tag{14.9}$$

See Eq. 14.12 for a more detailed expression for this correction.

Experiments indicate that the thickness of the free molecule region is equal to $2D/\langle v \rangle$. Since $D = \langle v \rangle \lambda/3$ from kinetic theory, we have

$$\delta = 2\lambda/3 \tag{14.10}$$

Namely, δ is of order of the mean free path. Using this relation, Eq. 14.9 can be rewritten as

$$\frac{\mathrm{d}m}{\mathrm{d}t} = \frac{(\mathrm{d}m/\mathrm{d}t)_D}{(4Kn/3\alpha) + 1/(1+2Kn/3)} \tag{14.11}$$

However, this equation tends to be incorrect for large Kn because of inaccuracy of Eq. 14.10. An improvement was made by Davis and Liao (1975) as follows ($\alpha \sim 1$).

$$\frac{\mathrm{d}m}{\mathrm{d}t} = 4\pi a D(c_\infty - c_a) \Big/ \left[1 + \frac{Kn(4Kn/3 + 0.71)}{1 + Kn}\right] \tag{14.12}$$

14.2 Particle Growth by Brownian Coagulation

As pointed before, if particles grow large (~ 0.1 nm) in size, coagulation processes become important for their further growth. We have discussed the particle growth, in Sec. 13.2 and Sec. 13.3.1, associated with the fractal structure of the particles and the sol-gel phase transition, respectively. But, here, we are directly concerned in the growth of the particle size, which is well demonstrated in coagulation processes in polydisperse systems.

14.2.1 Detailed Conditions in Coagulation Processes

In Sec. 11.2.1, we have discussed homogeneous coagulation in a monodisperse system, assuming that the particles are not lost in sedimentation due to collisions with a container wall. However, the treatment was in the continuous regime. In aerosols, the size of particles may be smaller than the mean free path of the surrounding gas molecules and corrections are needed accordingly.

We start here with the rate of homogeneous coagulation when $Kn \ll 1$.

$$\mathrm{d}n^0/\mathrm{d}t = -k(n^0)^2 \tag{14.13}$$

where n^0 is the number density of particles in the bulk, ignoring the developing polydispersity. The rate constant is given by Eqs. 11.9 and 11.11. Namely, $k = J/n^0$, where J is the number of particles reaching anyone of them per unit time, and

$$J = kn^0 = \frac{8k_\mathrm{B}T}{3\eta W} n^0 \tag{14.14}$$

with W defined by Eq. 11.14, or

$$W = 2a \int_{2a}^{\infty} \mathrm{e}^{\frac{\Delta G}{k_\mathrm{B}T}} \frac{1}{r^2 A_{11}} \mathrm{d}r \tag{14.15}$$

If $A_{11} = 1$ and the interparticle potential $\Delta G_\mathrm{T} = 0$, $W = 1$. By introducing the "slip" correction β_c (Eq. 11.33) for large Knudsen number, the k is replaced by

$$k_\mathrm{c} = k\beta_\mathrm{c} \tag{14.16}$$

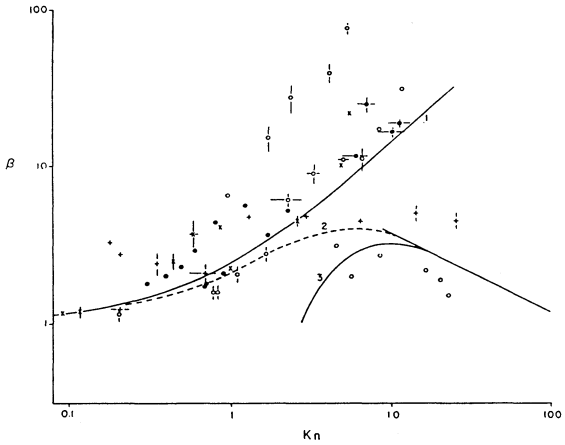

Fig. 14.2 Experimental values of β ($=k_{\text{corrected}}/k$) at various Knudsen number. Curve 1: $\beta=\beta_c$, curve 2: $\beta=\beta_c\beta_f$ [β_f: Fuch's correction (1934)], curve 3: β of Hidy and Brock (1965, 1970), the straight line for $Kn>10$: β due to a relative free molecule collision rate. Other symbols represent experimental data from 22 publications (Mercer, 1978, with permission from Wiley).

with

$$\beta_c = 1 + Kn(1.257 + 0.400e^{-1.10/Kn}) \tag{14.17}$$

As particle size approaches molecular dimensions, the rate constant must be further corrected. This is due to the discontinuity near the particle surface which was suggested by Langmuir (1915). Fuchs (1934) assumed that within a characteristic separation distance δ, particles of mass m move as if in a vacuum, i.e., in straight lines at their mean thermal speed $\langle v\rangle$ but with their effective mean free path λ_p ($=m\langle v\rangle/6\pi\eta a$). His additional correction factor is given by

$$\beta_f = \left[\frac{2a}{2a+\delta} + \frac{2\sqrt{2}D}{a\langle v\rangle}\right]^{-1} \tag{14.18}$$

where

$$D = \frac{k_B T}{6\pi\eta a} \quad \text{and} \quad \delta \approx \frac{\sqrt{2}}{6a\lambda_p}[(2a+\lambda_p)^3 - (4a^2+\lambda_p^2)^{3/2}] - 2\sqrt{2}a$$

Thus, the total correction amounts $\beta=\beta_c\beta_f$. This β is shown by curve 2 in Fig. 14.2, together with the correction calculated on extended free molecular theory by Hidy and Brock (1965, 1970). The extended theory includes interactions between two approaching particles only through the streams of gas molecules reflected or 'emitted' from each particle. The interactions provide an apparent repulsive force which retards coagulation. This correction is represented by curve 3 in Fig. 14.2. For $Kn>10$, this correction is similar to Fuch's.

If surface losses of particles are allowed, Eq. 14.13 should read

$$-\frac{\mathrm{d}n^0}{\mathrm{d}t} = k(n^0)^2 + \lambda_\mathrm{s} n^0 \tag{14.19}$$

where λ_s is a rate constant for surface losses. Assuming that k and λ_s are constant in time, integration yields

$$\frac{1}{n^0} = \left(\frac{1}{n_0} + \frac{k}{\lambda_\mathrm{s}}\right)\mathrm{e}^{\lambda_\mathrm{s} t} - \frac{k}{\lambda_\mathrm{s}} \tag{14.20}$$

If $Kn > 0.01$, similar corrections as discussed before are required.

However, if the polydispersity develops, theoretical predictions need to include the change of particle sizes during coagulation processes. We must then solve, in the continuum regime,

$$\frac{\partial n^0(v,t)}{\partial t} = k\left[\int_0^{v/2} \beta_{v',v-v'} n^0(v-v',t) n^0(v',t)\mathrm{d}v' - n^0(v,t)\int_0^{\infty} \beta_{v,v'} n^0(v',t)\mathrm{d}v'\right] - \lambda_\mathrm{s} n^0(v,t) \tag{14.21}$$

where $k = 4k_\mathrm{B}T/3\eta$, v, v' and v'' are particle volumes ($4\pi a^3/3$, $4\pi a'^3/3$, and $4\pi a''^3/3$, respectively), and $\beta_{v',v''}$ and $\beta_{v,v'}$ represent the volume-dependent corrections $\beta_\mathrm{c}\beta_\mathrm{f}$, corresponding to Eqs. 14.17 and 14.18. These corrections are written in terms of particle radii. For polydisperse systems, by taking an average, we write

$$\beta_{v',v''} = \beta_{a',a''} = (a' + a'')\left[\frac{\beta_\mathrm{c}(a')}{a'} + \frac{\beta_\mathrm{c}(a'')}{a''}\right] \cdot \beta_\mathrm{f}(a',a'') \tag{14.22}$$

where β_f, Eq. 14.18, is used to obtain $\beta_\mathrm{f}(a',a'')$ by approximating

$$a = (a' + a'')/2\,, \quad D = (D' + D'')/2\,, \quad \langle v\rangle = [(\langle v'\rangle^2 + \langle v''\rangle^2)/2]^{1/2}$$

where v is a particle speed instead of the volume, and

$$\lambda_\mathrm{p} = \{[\lambda_\mathrm{p}^2(a') + \lambda_\mathrm{p}^2(a'')]/2\}^{1/2}$$

In order to rewrite Eq. 14.21 in terms of particle radii, we multiply both sides by $\mathrm{d}v$. Noting that

$$n(v)\mathrm{d}v = n(a)\mathrm{d}a\,, \quad n(v'')\mathrm{d}v = n(a'')\mathrm{d}a''\mathrm{d}v/\mathrm{d}v''$$

Since $\mathrm{d}v/\mathrm{d}v'' = a^2\mathrm{d}r/a''^2\mathrm{d}a''$

$$n(v'')\mathrm{d}v = n(a'')(a^2/a''^2)\mathrm{d}r$$

Therefore, Eq. 14.21 leads to

$$\frac{\partial n^0(a,t)}{\partial t} = \frac{k}{2}\left[\int_0^{a/2^{1/3}} \beta_{a',a-a'} n^0(a-a',t) n^0(a',t) \frac{a'^2}{(a-a')^2}\mathrm{d}a' - n^0(a,t)\int_0^{\infty} \beta_{a,a'} n^0(a',t)\mathrm{d}a'\right] - \lambda_s n^0(a,t) \tag{14.23}$$

Nelson et al. (1966), Greenfield et al. (1971), Nicolaon et al. (1972), Yoshida et al. (1975), and Okuyama et al. (1976) showed that Eq. 14.23 gave good predictions of experimental data, including the size distributions as a function of time. However, they ignored β_f. Their observations included the mean Knudsen number less than 0.2. Husar (1971), on the other hand, reported average coagulation rate constants for the mean Knudsen numbers in the range of 5–35. He rewrote Eq. 14.21 to summations over the discrete particle size and his theoretical size distribution was found to be in good agreement with experiments.

14.2.2 Growth due to Coagulation

In Eq. 14.21, $n^0(v,t)$ represents the number density of particles of size v by volume in the bulk at time t. This may be denoted by n_k, where k is the number of molecules (monomers) in the particle of radius a_k. The population balances in time describe the particle growth. They are given by Eq. 14.21 or by the conservation equation, considering that the particle sizes are discrete:

$$\frac{\mathrm{d}n_k}{\mathrm{d}t} = \frac{1}{2}\sum_{i=1,j=k-i}^{k-1} J_{ij} - \sum_{i=1}^{\infty} J_{ki} \tag{14.24}$$

with $n_1(0)=n_0$ and $n_k=0$ for $k>1$, where, from Eqs. 14.14 and 14.22, if J refers to the total number of encounters per unit time per unit volume, instead of the number of encounters with a specific center particle,

$$J_{ij} = \frac{2k_B T}{3\eta W_{ij}}(a_i + a_j)\left(\frac{\beta_c(a_i)}{a_i} + \frac{\beta_c(a_j)}{a_j}\right)\cdot \beta_f(a_i,a_j) n_i n_j \tag{14.25}$$

Here, W_{ij} is usually approximated by the stability ratio, Eq. 11.19. Equation 14.24 can be numerically solved.

Measurements of particle size distribution as functions of time for polystyrene in 1.25 M KCl solution were obtained with a Coulter counter by Higashitani and Matsuno (1979). They found that the theory predicted quite accurately the growth of polystyrene particles. However, the particles thus produced must be fractals and the size k must be considered as a degree of aggregation defined by

$$k = (a_k/a_1)^D \tag{14.26}$$

14.3 Coagulation in Shear Flows

Experimental observations are usually made in a flowing system at Reynolds numbers such that Poiseuille flow is assured. Then, it is necessary to consider collisions brought about by the flow itself. A particularly important case is that of the presence of shear. This is called gradient coagulation for aerosols, which causes an additional complication to the coagulation discussed in Sec. 11.2.1. In the continuum regime, if there is no shear, the collision cross-section may be simply $\pi(2a)^2$ for two identical spherical particles of radius a, ignoring hydrodynamic interactions. But, if shear is present, the flow velocity varies over the cross-sectional area. Consider an xy plane passing through the center of a spherical particle of radius a which is subject to coagulation with approaching particles also of radius a. Suppose that the medium fluid flows in the x-direction with a shear rate $\mathrm{d}v/\mathrm{d}z$ in the z direction without being disturbed by the presence of dispersed particles. Ignoring Brownian motion and interparticle interactions, the approaching particles are assumed to move following the fluid streamline, so that their velocity is in the x-direction with magnitude $(\mathrm{d}v/\mathrm{d}z)z$ at a height z. Then, the collision rate of the center particle with approaching particles at the height between z and $z+\mathrm{d}z$ is given by

$$2(\mathrm{d}v/\mathrm{d}z)z \cdot [(2a)^2 - z^2]^{1/2}\mathrm{d}z$$

since the cross-sectional area element for this collision is $2[(2a)^2-z^2]^{1/2}\mathrm{d}z$ for two particles colliding at the height between z and $z+\mathrm{d}z$. If the system is polydisperse, $(2a)$ must be replaced by the sum of the radii of the two colliding particles. By integrating over the cross-section of the central particle, the number of particles reaching the central one per unit time is given by

$$J_\mathrm{s} = 4n^0 \int_0^{2a} \frac{\mathrm{d}v}{\mathrm{d}z} z[(2a)^2 - z^2]^{1/2}\mathrm{d}z = \frac{32}{3} n^0 a^3 \frac{\mathrm{d}v}{\mathrm{d}z} \tag{14.27}$$

This is Smoluchowski's equation for shear coagulation (Smoluchowski, 1917).

However, there are hydrodynamic interactions between the approaching and the center particle. The interactions oppose the relative velocity due to the imposed shear, pushing the spheres apart during the approach but pulling them together during separation. Batchelor and Green (1972) theoretically predicted closed trajectories around the central particle in a shear flow. Takamura, et al. (1981) observed the trajectories with a travelling microtube apparatus and a high-speed movie camera. Particles were 2.6 μm diameter polystyrene latex spheres and the conditions were chosen to minimize non-hydrodynamic forces.

When Brownian motion of particles are noticeable, the coagulation rate in a shear flow is characterized by a Peclet number, a measure of the strength of the flow relative to the Brownian motion. This is defined by

$$Pe = \frac{3\pi\eta a^3}{k_B T} \frac{\mathrm{d}v}{\mathrm{d}z} \tag{14.28}$$

(Compare the definition of Eq. 12.8.)

A. If $Pe \ll 1$, shear only slightly perturbs the Brownian coagulation. According to Van de Ven and Mason (1977), the number of particles reaching the central one per unit time is, instead of Eq. 14.14,

$$J = \frac{8k_B T n^0}{3\eta W}\left[1 + 0.257\frac{Pe^{1/2}}{W} + O(Pe)\right] \tag{14.29}$$

where W is given by Eq. 11.14. The coefficient, 0.257, owes Russel et al. (1989).

B. If $Pe \gg 1$, shear-induced coagulation is primary, but perturbed slightly by the Brownian contribution. Feke and Schowalter (1983) presented a theory for this case by assuming that the interparticle interactions were only of van der Waals' type with a Hamaker constant A. According to them, the rate of particle encounters per particle can be written in the form:

$$J = a^3 n^0 \frac{\mathrm{d}v}{\mathrm{d}z}\left(j_0 + \frac{j_1}{Pe} + \frac{j_2}{Pe^2} + \cdots\cdots\right) \tag{14.30}$$

where j_0 stands for no Brownian contribution. Since hydrodynamic interactions between the approaching particles affect their motion, they do not necessarily follow the fluid streamlines (Van de Ven and Mason, 1976), and Eq. 14.27 is satisfied only under a certain condition. Namely, when the flow number Fl defined by, with the Hawaker constant A,

$$Fl = \frac{6\pi\eta a^3}{A} \frac{\mathrm{d}v}{\mathrm{d}z} \tag{14.31}$$

is about unity (the flow strength is nearly equal to the attractive force), the relation Eq. 14.27 holds, so that $j_0 = 32/3$. In fact, the theory of Feke and Schowalter (1983) show a strong dependence of j_0 on Fl. The value of j_0 is about 20 for $Fl \sim 0.1$, and about 1 for $Fl \sim 10^4$. Similarly, $j_1 \sim 370$ for $Fl \sim 1$, $j_1 \sim 0$ for $Fl \sim 5 \cdot 10^2$, and $j_1 \sim -10^3$ for $Fl \sim 2 \cdot 10^4$. It is surprising that j_1 is negative if A is very small compared with the fluid flow strength. Thus, a little Brownian motion can either enhance or reduce the rate of coagulation.

Experimental results obtained in a Couette flow at shear rates between 200 to 1600 s^{-1} by Feke and Schowalter (1986) matched the prediction, within experimental error, for shear rates greater than 600 s^{-1} ($Pe \geq 60$).

14.4 Evaporation of Aerosols

In the continuum regime, Eq. 14.5 holds for evaporation of drops of not very volatile liquids if $c_a > c_\infty$, i.e.,

$$dm/dt = -4\pi a D(c_a - c_\infty) \tag{14.32}$$

If the drop is fairly volatile it cools while evaporating. Being cooler than the surrounding air, heat is conducted to it from air. If the drop does not move in air, the heat flows obeying

$$\frac{\partial T}{\partial t} = \frac{k_T}{s\rho}\left(\frac{2}{r}\frac{\partial T}{\partial r} + \frac{\partial^2 T}{\partial r^2}\right) \tag{14.33}$$

where k_T is the thermal conductivity of air, s is its specific heat, and ρ is its density. The diffusion coefficient D of vapor in air, which depends on the distance from the drop, may be approximated by

$$D = (D_a D_\infty)^{1/2} \tag{14.34}$$

Remember that the correction β is on the diffusion coefficient.

Since the flux of evaporating vapor at the drop surface is $D(dc/dr)_a$, the rate of heat loss by evaporation with a drop is $4\pi a^2 LD(dc/dr)_a$, where L is the latent heat of evaporation of liquid per unit mass. If this rate is equal to the heat conducted through air per unit time,

$$k_T\left(\frac{dT}{dr}\right)_a + LD\left(\frac{dc}{dr}\right)_a = 0 \tag{14.35}$$

Then we have

$$\left(\frac{\mathrm{d}c}{\mathrm{d}r}\right)_a = -\frac{1}{a}(c_a - c_\infty) = -\frac{m_v}{ak_\mathrm{B}}\left(\frac{p_a}{T_a} - \frac{p_\infty}{T_\infty}\right) \tag{14.36}$$

where the last expression is from Exercise 14.6 with m_v the mass of the vapor molecule. For a steady state, $\partial T/\partial t = 0$, from Eq. 14.33

$$\left(\frac{\mathrm{d}T}{\mathrm{d}r}\right)_a = -\frac{1}{a}(T_a - T_\infty) \tag{14.37}$$

Hence, the temperature depression when the steady state is reached is given by (Exercise 14.7)

$$T_\infty - T_a = \frac{LDm_v}{k_\mathrm{T}k_\mathrm{B}}\left(\frac{p_a}{T_a} - \frac{p_\infty}{T_\infty}\right) \tag{14.38}$$

Note that this does not depend on the drop size. This is fundamental to the wet bulb thermometer which is used for measuring atmospheric humidity.

The value of T_a may be estimated by using Eq. 14.38. Assuming equilibrium, p_a can be expressed in terms of T_a (Exercise 3.2). Therefore, Eq. 13.38 provides the value of T_a. A final adjustment can be made by approximation: $LD/k_\mathrm{T} = [(LD/k_\mathrm{T})_a(LD/k_\mathrm{T})_\infty]^{1/2}$, an application of the procedure of Eq. 14.34. Accordingly, c_a can be found.

If a very small droplet or particle is evaporating, Eq. 14.12 must then be used instead of Eq. 14.32. The adjustment of the kind of Eq. 14.34 for the variation of D may be made between $r = a + \delta$ and ∞.

When there is relative velocity v between a drop and air, the rate of mass transfer and that of heat become convective. However, there is no general solution to this problem.

If the droplet is uniformly receiving heat from surroundings at T_∞ by radiation, the rate of heat flow is $4\pi a^2\sigma({T_\infty}^4 - {T_a}^4)$ to the droplet, where σ is the Stefan-Boltzmann constant. This will promote the evaporation (Exercise 14.9).

14.5 Thermophoresis

Phoretic forces are forces which arise from the existence of ordered fluxes superimposed upon the disordered molecular motions in a gas. The flux may be a heat flux.

If there is a temperature gradient in an aerosol, the particles are exposed to a force due to the unbalanced momentum transfer from the surroundings. This ef-

fect is called thermophoresis, if no concentration gradients exist due to the temperature gradients. The thermal force may be used to collect aerosol particles for analysis (a thermal precipitator). It causes the deposition of airborn dust, soot, etc., on the cooler walls behind heat radiators.

The basic theory owes Maxwell, as discussed by Jacobson and Brock (1965). Knowing the velocity distributions of vapor and gas molecules around a particle, the momentum transfer to the particle per unit time is calculated. But much complexity exists to specify the velocity distributions, particularly, in the transition regime. In the free molecule regime ($Kn \to \infty$), the force on the particle of radius a was given by

$$\boldsymbol{F} = -\frac{32}{15} a^2 k_g \left(\frac{\pi m_v}{k_B T}\right)^{1/2} \nabla T \tag{14.39}$$

by assuming that the presence of the particles does not affect the gas temperature distribution. Here k_g is the thermal conductivity of the gas and the quantity $(\pi m_v/k_B T)^{1/2}$ is the average speed of the gas molecules, assumed to be monatomic. In practice, the formula is good to 5% down to $Kn = 10$ and only 10% even for $Kn \sim 5$. But, for $Kn \sim 0.25$, it was empirically found that

$$\boldsymbol{F} = \boldsymbol{F}_{\text{Eq.14.39}} e^{-\kappa/Kn} \tag{14.40}$$

This was theoretically obtained by Brock (1967). The value of κ depends on the aerosol system, with values near 0.5. For smaller Kn, the effect is rather small, but the analysis becomes hard.

The experimental methods of measuring the thermal force may be made by using the Millikan-type apparatus using charged aerosol particles by using a balancing electric field. Another method developed by Derjaguin et al. (1966) for a small temperature gradient ($\sim 3^\circ$C/cm) is to measure the particle velocity under a microscope. Results obtained by this method differ from the above prediction by a factor of two or three (in the theoretically difficult transition regime, where Kn was 0.15), indicating some inadequacy in the Maxwell's theory.

14.6 Diffusiophoresis

Diffusiophoresis occurs when a concentration gradient exist in a gas at constant temperature. It is observed in the vicinity of an evaporating drop, which causes drift of particles. Such a drift is involved in reducing the number of aerosol particles in the neighborhood of an evaporating droplet or liquid, causing a "dust free space" to be observed.

If there are concentration gradients in a gas mixture at constant temperature, there is an imbalance in the momentum transfer to particles and a (phoretic) force

appears. When water vapor diffuses along a direction, say, the x-axis, air may also diffuse if the system is at constant pressure. Thus, in order to describe the diffusive fluxes fully, we must consider that the fluxes satisfy

$$F_1 = D_1(\mathrm{d}n_1/\mathrm{d}x) + D_{12}(\mathrm{d}n_2/\mathrm{d}x)$$
$$F_2 = D_{21}(\mathrm{d}n_1/\mathrm{d}x) + D_2(\mathrm{d}n_2/\mathrm{d}x)$$
$$\mathrm{d}p/\mathrm{d}x = k_\mathrm{B}T[(\mathrm{d}n_1/\mathrm{d}x) + (\mathrm{d}n_2/\mathrm{d}x)]$$

where the two species are denoted by 1 and 2. Thus, the diffusion causes a pressure gradient.

If there is in air a volatile drop (of, say, water) nearby an aerosol particle, air may be sucked into the gap between the drop and the particle as the vapor evaporating from the drop diffuses away and the resulting concentration gradients cause repulsion between them. Experiments show that a dust-free space is found around evaporating drops, even though the dust particles are certainly below 1 μm. A theory for this phenomenon appears in Hidy and Brock (1970). The theory predicts that submicron particles should be collected by evaporating drops whereas larger particles should be collected by drops which are growing by condensation (Twomey, 1977).

14.7 Particle Capture

Elementary considerations show that a strong attractive force is necessary if freely suspended particles are to come together, because at close separations viscous resistance increases dramatically. Thus, capture of particles is particularly sensitive to the balance between interparticle and hydrodynamic forces. In gases the continuum approximation often begins to break down at length scales where interparticle forces are just coming into play.

14.7.1 Capture Efficiency and Filter Coefficient

Consider the deposition of aerosol particles of radius a on the surface of obstacles of size a_c, which work as a collector. Suppose that obstacles are uniformly packed in a plane sheet of thickness x and aerosol particles move with an average speed U toward the sheet perpendicularly. If the average number density of the particle is denoted by n, n decreases as the particles proceed in the direction of x because particles are collected by obstacles in the sheet. Since the flux J is given by nU,

$$\mathrm{d}J/\mathrm{d}x = U\mathrm{d}n/\mathrm{d}x = -\lambda J = -\lambda nU \tag{14.41}$$

The parameter λ is called the filter coefficient. We have

$$n = n_0 e^{-\lambda x} \tag{14.42}$$

The filter coefficient is related to the capture efficiency η as follows. If the particle size a is very small ($a \ll a_c$), then each obstacle has a cross-sectional area σ_c ($=\pi a_c^2$). Since each obstacle captures a fraction η of incident particles, the total fraction per unit length along the flow is

$$\lambda = \eta \sigma_c N \tag{14.43}$$

where N is the number density of obstacles. Here we have assumed that N is small and when the separation between the surfaces of a particle and a collector (obstacle) is a few Ångstroms a permanent bond is formed and the particle is captured.

14.7.2 Capture by a Sphere

The capture efficiency can be discussed in a microscopic model as follows. A simple treatment is to assume that particles move following the gas flow velocity $\boldsymbol{U}$ and the gas is an incompressible fluid, so that $\nabla \cdot \boldsymbol{U} = 0$. If the geometry of the flow is two-dimensional, then a function $\psi(x, y)$ can be introduced, such that

$$U_x = \frac{\partial \psi}{\partial y} \quad \text{and} \quad U_y = -\frac{\partial \psi}{\partial x} \tag{14.44}$$

This function is called the stream function, which automatically satisfies the continuity relation, $\nabla \cdot \boldsymbol{U} = 0$, in a steady flow.

Equation 14.44 can be written in spherical coordinates (r, θ, ϕ), if the polar axis is chosen in the direction of the main fluid flow,

$$U_r = \frac{1}{r^2 \sin\theta} \frac{\partial \psi}{\partial \theta} \quad \text{and} \quad U_\theta = -\frac{1}{r \sin\theta} \frac{\partial \psi}{\partial r} \tag{14.45}$$

In cylindrical coordinates (ρ, ϕ, z), if the flow is perpendicular to an infinitely long cylinder along the z direction,

$$U_\rho = \frac{1}{\rho} \frac{\partial \psi}{\partial \phi} \quad \text{and} \quad U_\phi = -\frac{\partial \psi}{\partial \rho} \tag{14.46}$$

We must consider that the stream function for the last case is per unit length in the direction of the symmetry axis of the cylinder. The azimuthal angle ϕ is measured from the direction of the main flow (the x direction).

From Eq. 14.44, it follows that any gas molecule flows along a line, called a streamline given by

$$\psi(x, y) = \text{a constant.} \tag{14.47}$$

The local flow velocity $\boldsymbol{U}$ is tangential to the streamline. If the value of the constant is varied, all the streamlines standing for the gas flow can be obtained. If inertia, interparticle interactions, diffusion, and buoyancy can be ignored, the motion of particles in the gas follows these streamlines. If they cannot be ignored, see following sections.

For slow, axisymmetric flow past a sphere (collector) of radius a_c we have, in the spherical coordinates with origin at the center of the sphere (Happel and Brenner, 1973, p. 123)

$$\psi = \frac{1}{4} U_\infty a_c^2 \left[\frac{a_c}{r} - 3\frac{r}{a_c} + 2\left(\frac{r}{a_c}\right)^2 \right] \sin^2\theta \tag{14.48}$$

This is called the Stokes stream function for the flow past a sphere. It depends entirely on the kinematical assumption of incompressibility, so that this stream function can arise in viscous fluid motions. Therefore, this Stokes stream function can provide an approximate means of computing drag forces on a sphere and a pressure distribution in a fluid flow ($\nabla p = \eta_v \nabla^2 \boldsymbol{U}$, p and η_v being the pressure and the viscosity of the fluid, respectively).

If the fluid flow is irrotational, so that $\nabla \times \boldsymbol{U} = \boldsymbol{0}$, $\boldsymbol{U}$ has a potential function φ such that $\boldsymbol{U} = \nabla\varphi$. Such a flow is called a potential flow. It occurs when the fluid viscosity or interparticle interactions can be ignored or outside of a boundary layer when the Reynolds number is large. In addition, if the fluid is incompressible, $\nabla^2\varphi = 0$. If we solve this Laplace equation for a flow passing a sphere, we have

$$U_r = U_\infty \cos\theta \left(1 - \frac{a_c^3}{r^3}\right) \quad \text{and} \quad U_\theta = -U_\infty \sin\theta \left(1 + \frac{a_c^3}{2r^3}\right) \tag{14.49}$$

From this the potential stream function can be found:

$$\psi = \frac{1}{2} U_\infty r^2 \left(1 - \frac{a_c^3}{r^3}\right) \sin^2\theta \tag{14.50}$$

(Russel et al., 1989, p. 28). The streamlines behave like lines of electric field around a sphere depicted in Fig. 10.7. The symmetry axis z is in the direction to the main flow direction U_∞.

The streamline, either potential or Stokes', is cylindrically symmetric about the main flow (here we choose the x axis along the symmetry axis following the convention used in Sec. 14.7.1). The streamlines corresponding to the same value of the constant (the same value of ψ) form a surface of a stream tube, which is

cylindrically symmetric about the x axis. The instantaneous volumetric flow rate within the cylinder must be the same throughout the tube. If the streamlines along the tube surface pass through a point at $r=a_c+a$ and $\theta=\pi/2$, particles following these streamlines just touch the collector at a grazing angle. Such a stream tube bounded by the grazing streamlines is called the grazing stream tube and particles which are captured must be those which flow through the region within this tube. The volume of fluid flow within this grazing tube per unit time is 2π times the value of the grazing stream function. Therefore, the number of the particles which are captured per unit time is given by $2\pi\psi_{\text{Grazing}}n$ (Exercise 14.11).

If we use Eq. 14.50, the grazing stream function has the value

$$\psi_{\text{Grazing}} = \frac{1}{2}a_c^2 U[(1+\alpha)^2 - 1/(1+\alpha)], \quad \alpha = a/a_c \tag{14.51}$$

Thus, the capture efficiency for a potential flow is

$$\eta = (1+\alpha)^2 - 1/(1+\alpha) \to 3\alpha \quad \text{for} \quad \alpha \ll 1 \tag{14.52}$$

If we use Eq. 14.48, the efficiency for a Stokes flow is given by

$$\eta = (1+\alpha)^2 - (3/2)(1+\alpha) + (1/2)(1+\alpha)^{-1} \to (3/2)\alpha^2 \tag{14.53}$$

As described before, this is good even for a viscous fluid.

We see that if the particle is smaller, it is harder to be collected by the above deposition process (see Sec. 14.8.2 for Brownian particles).

14.7.3 Capture by a Cylinder (Fibrous Filter)

Fibrous filters are at present the most perfect and economical method of fine purification of air. Fibrous material is a system of variously oriented fibers with a preferred orientation across the direction of flow. The fiber diameter varies from 10^2 to 10^{-2} μm.

Assume that a cylindrical collector of radius a_c is infinitely long and placed perpendicularly to the main stream direction. There is no solution of Eq. 14.46, which satisfies simultaneously the boundary conditions at the cylinder surface (stick conditions) and approaches a uniform flow U_∞ far from the collector. The Stokes' stream function which diverges least rapidly as $\rho \to \infty$ is (Rosenhead, 1963)

$$\psi = \frac{U_\infty a_c}{2k_0}\left(\frac{a_c}{\rho} - \frac{\rho}{a_c} + 2\frac{\rho}{a_c}\ln\frac{\rho}{a_c}\right)\sin\phi \tag{14.54}$$

where k_0 is a constant, which depends on the boundary conditions on the outer expansion of the stream function, which may be determined by the Reynolds

number in the main flow or by the presence of surrounding fibers in the filter system.

If a cylindrical collector is isolated, $k_0 = 2 - \ln Re$, Re is the Reynolds number $\rho_g U_\infty (2a_c)/\eta_g$ (ρ_g, η_g: gas density and viscosity). On the other hand, the fluid flow in a fiber system is separately confined in the neighborhood of each fiber. For simplicity, consider that fibers are parallel each other. The flow of fluid in the volume around each fiber may be treated separately. The boundary conditions between the neighboring fluid volumes are such that the normal velocity component and the vorticity vanish at the boundaries. Introducing the packing density φ (fiber volume fraction) related to the fluid volume around each fiber and, therefore, to porosity of the fiber system $\beta = 1 - \varphi$, Kuwabara (1959) obtained

$$k_0 = -0.5 \ln \varphi - 0.75 + \varphi - 0.25\varphi^2 \tag{14.55}$$

The reason why this does not contain the Reynolds number is that Stokes' equation is used to describe the fluid flow within each fluid volume.

We have discussed slippage of gas when the mean free path of gas molecules are comparable with the particle radius. If so, the tangential velocity component U_ϕ is not equal to zero on the fiber surface. Therefore, the stream function must be found with the boundary condition:

$$(U_\phi)_{\rho = a_c} = -\tau Kn \left(\frac{\partial U_\phi}{\partial \rho} \right)_{\rho = a_c} \tag{14.56}$$

where τ is a coefficient of order of unity and depends on interaction of gas molecules and the fiber surface. This boundary condition is an approximation for $Kn \ll 1$ (possibly $0.01 < Kn < 0.25$). According to Kirsch and Stechkina (1978) the stream function near the cylinder is approximately given by

$$\psi = \frac{U_\infty a}{2(k_0 + \tau Kn)} \left[(1 - 2\tau Kn) \left(\frac{a_c}{\rho} - \frac{\rho}{a_c} \right) + 2 \frac{\rho}{a_c} \ln \frac{\rho}{a_c} \right] \sin \phi \tag{14.57}$$

where k_0 is a constant when $Kn = 0$. Then, the capture efficiency is given by

$$\eta = \frac{1}{2(k_0 + \tau Kn)} \left[\frac{1}{1 + \alpha} - (1 + \alpha) + 2(1 + \alpha) \ln(1 + \alpha) + 2\tau Kn \frac{(2 + \alpha)\alpha}{1 + \alpha} \right] \tag{14.58}$$

For $\alpha = a/a_c \ll 1$,

$$\eta \to \frac{\alpha^2}{2(k_0 + \tau Kn)} \left(1 + \frac{2\tau Kn}{\alpha} \right) \tag{14.59}$$

For the transition regime ($0.25 < Kn < 10$), according to Davis (1966)

$$\psi = \frac{U_\infty a}{2k_0}\left[\frac{a_c}{\rho}f(Kn) - \omega\frac{\rho}{a_c}(1 + k_1 Kn)^2 + 2\frac{\rho}{a_c}\ln\frac{\rho}{a_c(1 + k_1 Kn)}\right]\sin\phi \tag{14.60}$$

where $f(Kn) = \omega(8Kn+1)$, with $\omega = (2Kn+\frac{1}{2}\beta)/(2\beta Kn+Kn+\frac{1}{2}\beta)$ and $\beta = 1+\frac{1}{4}\pi$, and k_1 is a dimensionless constant of order unity. For $Kn \to 0$ Eqs. 14.57 and 14.60 are reduced to Eq. 14.54.

The problem of determining the flow field in a fibrous filter composed of cylindrical particles is much more complex and has been solved only approximately by Happel (1959), Kuwabara (1959), and Spielman and Goren (1968). All these models are based on the assumption that Stokes' equation can be applicable to slow fluid motion. This is the case when the neighboring fibers are sufficiently close to each other ($\varphi > 0.01$). In this case the inertia effect may also be small. Spielman and Goren (1968) considered various cases of fiber arrangements, including the case that all fiber axes oriented in planes perpendicular to the flow direction with completely random in each plane. When $Kn \ll 1$ (no slip on the fiber surfaces), the stream function of Eq. 14.54 can be used with

$$k_0 = \frac{K_0(s)}{sK_1(s)}, \quad \varphi = \frac{1}{2}\left(1 + 2\frac{K_1(s)}{sK_0(s)}\right)^{-1} \tag{14.61}$$

where $K_0(s)$ and $K_1(s)$ are the modified Bessel functions of order 0 and 1, respectively. The value of s may be obtained by knowing the fiber volume fraction φ and then the flow parameter k_0 can be found.

14.8 Effects of Inertia, Interactions, Diffusion on Capture Efficiency

Particles do not necessarily follow the streamlines of gas flow if particles have mass m or if they are subjected to hydrodynamic and interparticle interactions or to Brownian motion. Accordingly, the capture efficiency must depend on inertia, interactions, and diffusion of particles.

14.8.1 Inertia and Hydrodynamic and Interparticle Interactions

It is interesting that there is an inertia threshold below which capture is impossible unless interparticle attractive forces are present. If particles move with a differ-

ent velocity $d\boldsymbol{r}/dt$ from the gas flow velocity $\boldsymbol{U}(\boldsymbol{r})$, a viscous force $6\pi\eta_g a[(d\boldsymbol{r}/dt)-\boldsymbol{U}(\boldsymbol{r})]$ is exerted on the particles. If the mass of the particle is denoted by m, the equation of motion is given by

$$m\frac{d^2\boldsymbol{r}}{dt^2} = -6\pi\eta_g a\left[\frac{d\boldsymbol{r}}{dt} - \boldsymbol{U}(\boldsymbol{r})\right] \tag{14.62}$$

Consider a spherical collector. Experimental data (in the range of the Reynolds number (Re) from 100 to 330) of Wong and Johnstone (1953) agree with the theory of particle capture in an inviscid flow (Brun et al., 1955). (The Reynolds number is defined by $Re=\rho_g U_\infty(2a_c)/\eta_g$.) Therefore, for simplicity, let us use Eq. 14.49 of a potential flow to evaluate $\boldsymbol{U}(\boldsymbol{r})$ in Eq. 14.62. For the flow towards a sphere ($\theta=\pi$ and $U_r=-3U_\infty(r-a_c)/a_c$), Eq. 14.62 can be written as

$$C\frac{d^2y}{dt^2} + \frac{dy}{dt} + 3\frac{U_\infty}{a_c}y = 0\,, \quad \text{with} \quad C = \frac{m}{6\pi\eta_g a} \tag{14.63}$$

where $y=(r-a_c)/a_c$ is the distance upstream from the surface in the unit of a_c. The solution of this equation is ($C\neq 0$)

$$y = c_1 e^{-\frac{1}{2C}(1+\sqrt{1-12CU_\infty/a_c})t} + c_2 e^{-\frac{1}{2C}(1-\sqrt{1-12CU_\infty/a_c})t} \tag{14.64}$$

If $C=0$, $y=y_0e^{-t/\tau}$ ($\tau=a_c/3U_\infty$), and y decreases with time, where y_0 is the initial position, but never approaches zero in a finite time. This is because the particle velocity and the fluid velocity coincide because of no inertia. For $12CU_\infty/a_c<1$, the inertia is too small to overcome the viscous effect and the particle can never reach the surface. The quantity CU_∞/a_c is called Stokes' number (St), defining the threshold for the inertial capture.

For $12CU_\infty/a_c=12St>1$,

$$y = y_0 e^{-\frac{t}{2C}}\cos\left(\sqrt{\frac{12CU_\infty}{a_c}-1}\;t + c\right)/\cos(c) \tag{14.65}$$

The last case predicts that $y\to 0$ at a finite time t. An application of the stream function for a potential flow for low Re is questionable in real fluids. The above analysis neglects boundary layer effects, so that it will be best applied when the particle diameter is larger than the boundary layer thickness (see below). The change in the drag law as the particle approaches the surface is also not taken into account.

In order to introduce interactions between particles, by noting that $m/(6\pi\eta_g a)$ is a mobility of the particle and $md^2\boldsymbol{x}/dt^2$ is a force acting on the particle we can rewrite Eq. 14.62 as follows.

$$\frac{\mathrm{d}}{\mathrm{d}t}\boldsymbol{r} = \boldsymbol{U}(\boldsymbol{r}) + \overleftrightarrow{\boldsymbol{b}}(\boldsymbol{r}) \cdot \boldsymbol{F}(\boldsymbol{r}) \tag{14.66}$$

where $\boldsymbol{U}(\boldsymbol{r})$ is the local undisturbed fluid velocity, $\overleftrightarrow{\boldsymbol{b}}$ is the mobility tensor (see Eq. 4.74), and $\boldsymbol{F}(\boldsymbol{r})$ is the force on the particle. $\boldsymbol{F}(\boldsymbol{r})$ includes buoyancy, van der Waals' dispersion forces, and electrostatic forces (aerosols) or electric double-layer forces between the particle and the collector. The Hamaker constant may need a correction factor for large Kn which is given by, for $a \ll a_c$) (Suzuki et al., 1969)

$$F(y/a, Kn) = \frac{Kn(Kn + 22.23y/a)}{(y/a)^2(Kn + 11.12y/a)^2} \tag{14.67}$$

where y is defined by the shortest distance between the surfaces of the two spheres. Also see Eq. 8.5.

The variable t can be eliminated in Eq. 14.66, after separating into the r– (or ρ–) and θ– (or ϕ–) components, to find an equation of the trajectory of the particle. The equation may be numerically solved. If the attraction is strong, particles initially outside of the grazing stream tube can have trajectories which cross the surface of the tube and are captured by the collector. There is a limiting trajectory. Inside the limiting trajectory, all particle paths intersect the collector. If we trace this limiting trajectory back upstream, then it will coincide with a streamline, which has the stream function of a value ψ_l. We can write the capture efficiency for a spherical collector as

$$\eta = 2\frac{\psi_l}{a_c^2 U_\infty} \tag{14.68}$$

In order to find the value of the stream function on the limiting streamline, first we note that as long as we use Stokes' stream function it must have the form of Eq. 14.48 for a spherical collector. We rewrite it for a convenient form. If the shortest distance between the surfaces of the two spheres of radii, a_c and a, is denoted by y, $y = r - a_c - a$ and

$$\frac{r}{a_c} - 1 = \frac{a}{a_c}\left(\frac{y}{a} + 1\right) \tag{14.69}$$

Substituting this into Eq. 14.48 we have the approximate stream function:

$$\psi \approx \frac{3}{4}a_c^2 U_\infty \left(\frac{a}{a_c}\right)^2 \left(\frac{y}{a} + 1\right)^2 \sin^2\theta\,, \quad \frac{a}{a_c}\left(\frac{y}{a} + 1\right) \ll 1 \tag{14.70}$$

The capture efficiency follows from the limiting value of $\{(y/a)+1\}^2\sin^2\theta$ as $\theta \to \pi$. Thus,

$$\eta = \lim_{\theta \to \pi} (2/3)[(a/a_c)\{(y/a) + 1\} \sin\theta]^2 \tag{14.71}$$

A relation between y and θ for the limiting streamline may be obtained by finding the limiting trajectory from Eq. 14.66. Spielman and Goren (1970) obtained such a limiting trajectory from Eq. 14.66 and applied Eq. 14.71 for a spherical collector, but this result was a poor approximation since interparticle attraction and the viscous drag were not sufficiently included.

Electric charge on particles affects the force between particles. In the continuum regime, Spielman and Cukor (1973) predicted capture efficiencies by numerical integration of the trajectory equation.

14.8.2 Capture of Brownian Particles

The Brownian motion becomes more important as particle size decreases. As a result, the efficiency of collection by diffusion for smaller than 0.5 μm actually increases with decreasing particle size. On the other hand, we have seen in the last section that if particle size is large and particle is heavier, inertial effects are important and the capture efficiency increases with increasing size at a fixed flow velocity. In the efficiency curve against the particle size there is a "window" at particle size in the 0.1 to 1.0 μm range. A rigorous method of calculating the transition from the diffusion regime to the inertial regime has not been developed.

The aerosol concentration at large distances from the collector surface is usually uniform. But, within one particle radius from the surface, the concentration vanishes. If the flow velocity is large, it carries most of the particles past the collector. In the immediate vicinity of the collector, the diffusional process is important since the collector acts as a particle sink. Near the surface, the concentration thus drops sharply from the bulk value to zero. This surface region is known as the concentration (or diffusion) boundary layer. The boundary conditions for spherical particles are

$$\begin{aligned} &n = 0 \quad \text{at} \quad r = a + a_c \ , \\ &n \to n_\infty \quad \text{as} \quad r \to \infty \ . \end{aligned} \tag{14.72}$$

But, for simplicity, it is usually assumed that $a/a_c \ll 1$ and the particle size a does not appear explicitly in the formalism.

For the Brownian particles, the continuity equation assumes the usual form:

$$\frac{\partial n}{\partial t} + \nabla \cdot \boldsymbol{j} = 0 \tag{14.73}$$

where n is the particle number density. For a steady state, $\nabla \cdot \boldsymbol{U} = 0$ for incompressible fluid, where $\boldsymbol{U}$ is the flow velocity of the fluid, so that convective diffusion occurs. The particle flux $\boldsymbol{j}$ is given by

$$\boldsymbol{j} = \left(-\overleftrightarrow{D} \cdot \nabla \ln n + \frac{\mathrm{d}\boldsymbol{r}}{\mathrm{d}t}\right) n$$
$$= [\boldsymbol{U} + \overleftrightarrow{b} \cdot (-k_{\mathrm{B}} T \nabla \ln n + \boldsymbol{F}) - \overleftrightarrow{K}_{\mathrm{c}}^{\dagger} \cdot \overleftrightarrow{K}_{r}^{-1} \cdot \overleftrightarrow{b} \cdot \boldsymbol{T}] n \tag{14.74}$$

where $\overleftrightarrow{D}$ and $\overleftrightarrow{b}$ are the diffusion dyadic and the mobility dyadic, respectively, with $\overleftrightarrow{b} = (1/\eta_{\mathrm{g}})\overleftrightarrow{K}_{\mathrm{r}} \cdot (\overleftrightarrow{K}_{\mathrm{r}} \cdot \overleftrightarrow{K}_{\mathrm{t}} - \overleftrightarrow{K}_{\mathrm{c}}^{\dagger} \cdot \overleftrightarrow{K}_{\mathrm{c}})^{-1}$. The symbols $\overleftrightarrow{K}_{\mathrm{r}}$, $\overleftrightarrow{K}_{\mathrm{t}}$, and $\overleftrightarrow{K}_{\mathrm{c}}$ are the rotation, translation, and coupling dyadics († denotes the transpose), as defined by Happel and Brenner (1973, pp. 167 and 171). $\boldsymbol{F}$ is the forces including hydrodynamic forces, and $\boldsymbol{T}$ is the torque, respectively.

The mobility dyadic is known as a function of particle-collector separation only for a spherical particle near a rigid plane surface. It corresponds to hydrodynamic interactions and is tabulated in Brenner (1961), Bart (1968), Goldman et al. (1967), and Goren (1973). The hydrodynamic interactions for two identical spheres are discussed in Sec. 4.1.3. In most practical situations the particle size is much smaller than the size of the collector. Because the diffusion boundary layer thickness is usually comparable with the particle size, an assumption of a plane surface for the collector provides a good accuracy.

The total number of particles reaching the surface of the collector per unit time is

$$J = -\int_{S > S_{\mathrm{c}}} \boldsymbol{j} \cdot \boldsymbol{n} \mathrm{d}S \tag{14.75}$$

Here, $\boldsymbol{n}$ is the outward normal to the closed integration surface S enclosing the collector surface. Then, the capture efficiency is given by, for a spherical collector,

$$\eta = J / n\pi a_c^2 U_{\infty} \tag{14.76}$$

For a cylinder, the surface S of Eq. 14.75 is per unit length and the efficiency is given by

$$\eta = J / n 2 a_{\mathrm{c}} U_{\infty} \tag{14.77}$$

The simplest case that can be solved is the diffusional deposition of inertialess particles without hydrodynamic and interparticle interactions. We will consider a fibrous filter. With a constant (scalar) particle diffusivity D, since $\nabla \cdot \boldsymbol{j} = 0$, from Eq. 14.74

$$\nabla \cdot (\boldsymbol{U} n) = D \nabla^2 n \tag{14.78}$$

This is the convective diffusion equation. Since $\nabla \cdot \boldsymbol{U} = 0$ for an incompressible fluid, we have, for a cylindrical collector,

$$U_\rho \frac{\partial n}{\partial \rho} + U_\phi \frac{1}{\rho} \frac{\partial n}{\partial \phi} = D\left(\frac{\partial^2 n}{\partial \rho^2} + \frac{1}{\rho} \frac{\partial n}{\partial \rho} + \frac{1}{\rho^2} \frac{\partial^2 n}{\partial \phi^2}\right) \tag{14.79}$$

When $a_c U_\infty \gg D$, the transition from $n = n_\infty$ to $n = 0$ occurs within a thin layer near the surface (Exercise 14.16). Therefore, the stream function near a cylinder can be described by the first term in the expansion of Eq. 14.54 with respect to $\xi = (\rho/a_c) - 1$, i.e.,

$$\begin{aligned} &\psi = (U_\infty a_c / k_0)\xi^2 \sin\phi \\ &U_\rho / U_\infty = (1/k_0)\xi^2 \cos\phi\,, \quad U_\phi / U_\infty = -(2/k_0)\xi \sin\phi \end{aligned} \tag{14.80}$$

Using Eqs. 14.79 and 14.80, the thickness δ of the diffusion layer can be estimated as

$$\delta \sim a_c (2k_0/Pe)^{-1/3} \tag{14.81}$$

where Pe is the Peclet number defined by

$$Pe = 2U_\infty a_c / D = 12\pi \eta_g a a_g U_\infty / k_B T \tag{14.82}$$

where $2a_c$ is the diameter of the collector, a is the radius of the particles, and η_g is the viscosity of the gas, which depends on Kn. The above is an approximation for $a/a_c \ll 1$. If $a/a_c < 1$ or is larger, the boundary condition $n = 0$ at $\rho = a_c$ must be reexamined.

In calculating J, Eq. 14.75, we introduce a new variable $\zeta = \xi a_c/\delta$. From Eq. 14.79, we then approximately have

$$\begin{aligned} &\zeta^2 \cos\phi \frac{\partial n}{\partial \zeta} - 2\zeta \sin\phi \frac{\partial n}{\partial \phi} = \frac{\partial^2 n}{\partial \zeta^2}\,, \\ &n_{\zeta=0} = 0\,, \quad n_{\zeta\to\infty} = n_\infty\,, \quad n_{\phi=\pi}(\zeta) = \frac{1}{3^{1/3}\Gamma(1/3)} \int_0^\zeta e^{-\zeta^3/3} d\zeta \end{aligned} \tag{14.83}$$

$\Gamma(1/3)$ is the gamma function. This solution was obtained by Happel (1959). Then, since the outward normal component of the flux $\boldsymbol{j}$ to the cylindrical surface, $\rho = a_c$, is given by $D(\partial n/\partial \rho)$ at $\rho = a_c$, from Eq. 14.77 the capture efficiency has the value:

$$\eta = \frac{J}{n 2 a_c U_\infty} = \frac{2}{Pe} \int_0^\pi \left(\frac{\partial n}{\partial \frac{\rho}{a_c}}\right)_{\rho = a_c} d\phi = \frac{2}{2k_0 Pe^{2/3}} \int_0^\pi \left(\frac{\partial n}{\partial \zeta}\right)_{\zeta=0} d\phi \tag{14.84}$$

Or

$$\eta = 3.654(2k_0)^{-1/3} Pe^{-2/3} \tag{14.85}$$

The capture efficiency for spheres is given by Levich (1962).

$$\eta = 2.52 Pe^{-2/3} \tag{14.86}$$

Therefore, noting Eq. 14.82, in either a cylindrical or spherical collector, the efficiency increases as the particle size decreases and as the temperature increases, as Bell (1974) observed. But, the inertial effect becomes important for larger particles, as discussed before.

To account for interparticle forces and hydrodynamic effects on $\overleftrightarrow{D}(\boldsymbol{r})$, Eq. 14.74 must be integrated numerically. Adamczyk and Van de Ven (1981) treated an isolated cylindrical collector as well as a fibrous filter, taking rigorously into account specific surface interactions (dispersion and double-layer forces) and external forces (gravity and electrostatic) and obtained extensive results. Among them, the numerical calculations predict an appreciable increase in the deposition rate, up to an order of magnitude, when strong attractive double-layer forces are acting between the particle and the collector surface. These forces depend on the size of the particle and the collector. The Peclet number is defined by

$$Pe = 2U_\infty a^3/[(2 - \ln Re)a_c^2 D_\infty] \tag{14.87}$$

instead of the usual definition, $2U_\infty a_c/D_\infty$. The effects of the attractive forces are especially well pronounced in the region near the forward stagnation point and for values of the Peclet number larger than 10^{-2} (corresponding approximately to a particle of $a_c = 0.5$ μm diameter in water for $U_\infty = 0.1$ cm/s). For smaller particles, and in the region close to the rear of the collector (where the diffusion boundary layer becomes thick), the influence of colloidal forces becomes less important. For aerosols, the effect of the colloidal forces is less important in comparison with effects of external forces such as gravity and electrostatic forces (aerosol particles usually bear an electric charge). When a gravity force is acting parallel to the flow direction, the influence of colloidal forces ceases to be important for $Gr/Pe > 10^3$ and $Pe < 10^{-2}$, where $Gr = 4\pi(\rho_P - \rho_g)|\boldsymbol{g}|a^4/3k_BT$ is the dimensionless gravity number. In this case, the particle deposition is significant only for $\phi < \pi/2$. However, when the external force is directed antiparallel to the flow no such simple relationships are present and the effect of the dispersion and double-layer forces may be significant even for large Gr numbers. When the condition $GrD_\infty/U_\infty a \ll 1$ (similarly for electric forces) is fulfilled (usually the case in practice), the external force influences only slightly the deposition rate which becomes more uniform over the collector surface.

The gravity number is a quantity which is a measure of the strength of sedimentation under a gravitational body force of $O(4\pi(\rho_p - \rho_g)|\boldsymbol{g}|a^3/3)$ relative to the

Brownian force of $O(k_BT/a)$. But if the gravitational force is compared with the viscous force $O(6\pi\eta_g aU_\infty)$, it is called the sedimentation number.

For spherical collectors, Prieve and Ruckenstein (1974) show, for $a/a_c = 10^{-3}$ and an attraction, $10^{-4} < A_{eff}/k_BT < 10^2$, that the capture efficiency, Eq. 14.86, obtained by Levich (1962) ignoring the particle size and the interparticle force is a good approximation to their results at high Peclet number ($10^2 < Pe < 10^9$), where the diffusion boundary layer is much thinner than the attractive force. The deviations occur when the boundary layer thickness becomes comparable with the effective range of the attractive force and particles are captured from a layer much thicker than that subsumed by Levich (1962). Therefore, Levich's result underestimates the efficiency. For higher Pe numbers, the layer is too thin, so that the boundary layer theory gives too small values to the efficiency.

14.9 Scavenging by Falling Water Drops

The cleaning of the atmosphere by rainfall and the use of water spray are familiar examples of the phenomenon of capture of aerosol particles by falling water drops. In the atmosphere, aerosol particles are carried to ground by serving as nuclei for condensation of water vapor as well as capture. If aerosol particles are washed out by being captured by raindrops of radius a_j with number density N_j which falls with speed U_j, the number density of i-th aerosol particles decreases in time according to

$$n_i = n_i^0 e^{-\lambda_i t} \tag{14.88}$$

where

$$\lambda_i = \sum_j \eta_{ij} \pi a_j^2 N_j U_j \tag{14.89}$$

where η_{ij} is the important quantity both in theory and experiment. It is called the collection (capture) coefficient. Note that Eq. 14.89 contains the flow speed, contrary to Eq. 14.43. We have assumed that the aerosol particles are much smaller than a_j. The values of η_{ij} usually range between 10^{-5} and 10^{-2} and those of λ_i are 0.01 to 0.06 hr^{-1}, with higher values for smaller aerosols. The size distribution of actual raindrops is peaked at about 1-mm radius.

When removal processes of aerosols occur in precipitation (rain, snow, settling of fog droplets), they are classified as "wet" and also called "washout" processes. When aerosols are removed in the dry, particulate state, it is dry removal. The latter is observed with larger particles falling directly onto a surface or impaction, which operates in a similar way to that in impactor instrument, where curvilinear airflow occurs with sharp changes in direction near the surface, so that the larger particles are unable to follow the flow and subjected to impaction with the sur-

face. Likewise, in dry condition, aerosols must be transported, for the removal, to the surface of a water droplet by means of turbulence, i.e., random walks on a larger scale. Even if turbulent motions transport a particle close to the surface, it cannot complete the removal process. The particle must make the last step in some other ways such as inertial deposition, molecular diffusion, thermophoresis, diffusiophoresis, photophoresis, and/or strong interparticle interactions, which could be electrostatic.

The washout mechanism is either inertial deposition or convective diffusion on a falling drop or ice particle and equivalent to collection of moving particles by a stationary obstacle, which is discussed in previous sections. For potential flow the approximation $\eta = St$ is reasonably good, where St is the Stokes' number defined by $m_p U_\infty / 6\pi a \eta_g a_c$ or $2\rho_p a^2 U_\infty / 9\eta_g a_c$. Remember that the air viscosity η_g depends on the Knudsen number. The speed U_∞ may be the terminal speed of the falling water or ice droplet. Of course, the capture efficiency η cannot be greater than unity. For this maximum condition, since $U_\infty / a_c \approx 8300\ \mathrm{s}^{-1}$ at $a_c \approx 75\ \mu\mathrm{m}$, an efficient collection occurs for

$$\rho_p a^2 \geq 9\eta_g (8300)^{-1}/2 \approx 10^{-8}\ \mathrm{g/cm} \quad \text{or} \quad a \geq 10^{-4} \cdot \sqrt{(1/\rho_p)}\ \mathrm{cm} \tag{14.90}$$

Thus, with decreasing aerosol particle size, a rather abrupt transition from efficient collection to poor or no collection is expected below 1 μm. The efficiencies will be in the hundredth or thousandth of one percent category.

In heavy rain, the size of rain drops increases and a smaller value of U_∞ / a_c reduces the efficiency, but the flow pattern is viscous for small particles and becomes increasingly turbulent, so that the decrease in U_∞ / a_c is offset by the turbulent flow pattern.

If the particle size is a little below 1 μm, the collection efficiencies are so low that experimental measurements are very difficult. The determination of the particle size is also harder. But, experimental results obtained by Hampl et al. (1971) support the efficiency given by

$$\eta \simeq 1.68 Pe^{-2/3} \tag{14.91}$$

This is very close to Eq. 14.86. The drop size a_c used in the observation was 0.71, 0.94, and 1.16 mm and the value of $Pe = 2a_c U_\infty / D$ was in the $4 \cdot 10^7$ to $9 \cdot 10^7$ range.

For smaller aerosol particles, Friedlander (1967) approximately obtained

$$\eta = \frac{4}{Pe}(1 + 0.4 \cdot Re^{1/6} Pe^{1/3}) \tag{14.92}$$

This efficiency is simply the ratio of the number of particles diffusing to the drop to the number of particles in the volume swept out by the falling drop. It can ex-

ceed unity since particles outside the swept volume can reach the surface of the drop if their diffusions are large enough.

The efficiency of cloud removal processes for particles in most size ranges is high – in contrast to the situation for dry removal and removal by precipitation below cloud levels. The primary reasons for this are simply the very large surface area provided by the cloud droplets and the effect of condensation in transferring particulate material from a small size quite abruptly into a much larger size range. The latter is most effective when the particle is soluble.

Exercises

14.1 The static dielectric constant ε of air (dry) is 1.00054. Find the maximum amount of charge on a drop of water ($\gamma = 72\ \mathrm{mJm^{-2}}$) of radius 1 μm. What strength of the electric field is required to form this charged drop at the tip of a capillary?

14.2 Using Eq. 14.2, find the mean free path of air at 1 atm and 20°C. (Ans.: $\lambda \sim 9.8$ nm.)

14.3 Establish Eq. 14.5.

14.4 Does the coagulation rate of aerosols of noninteracting particles depend on the particle size? If so, show how to estimate the magnitude of the effect.

14.5 Is it possible to write an equation for the particle growth in polydisperse systems, so that it is directly related with the growth of a given particle?

14.6 Rewrite Eq. 14.32 in terms of vapor pressure and temperature, assuming that the vapor is almost a perfect gas. ($\mathrm{d}a^2/\mathrm{d}t = -(2D/\rho_\mathrm{l})(m_v/k_\mathrm{B})[(p_a/T_a) - (p_\infty/T_\infty)]$, where m_v is the mass of the vapor molecule and ρ_l is the liquid density.)

14.7 Is Eq. 14.38 modified if the heat capacity of the drop is taken into consideration and the thermal diffusivity ($k_\mathrm{l}/s_\mathrm{l}\rho_\mathrm{l}$) of liquid is much larger than that of air?

14.8 Calculate a general expression for the lifetime of a water droplet at rest by using the result of Exercise 14.6. Here assume that the temperature of the drop does not change during the evaporation and is constant at the initial steady state value, since the lifetime of an evaporating droplet of water is much longer than the time required to attain the steady state temperature. If the initial radius a_0 is 0.2 cm and the relative humidity is 80%, find the numerical value for the lifetime at 20°C. (Ans: $a_0 k_\mathrm{B}\rho_\mathrm{l}/[2Dm_v(p_a/T_a - p_\infty/T_\infty)]$)

14.9 Suppose that a liquid droplet of radius a is exposed to surroundings at T_∞ ($> T_\mathrm{a}$). If an appreciable heat flows into the droplet but the droplet temperature does not change, then how much does the rate of evaporation increase due to this heat flow?

14.10 From Eq. 14.48, obtain, in spherical coordinates,

$$U_r = \frac{1}{2} U_\infty \cos\theta \left[\left(\frac{a_c}{r}\right)^3 - 3\frac{a_c}{r} + 2 \right]$$

$$U_\theta = \frac{1}{4} U_\infty \sin\theta \left[\left(\frac{a_c}{r}\right)^3 + 3\frac{a_c}{r} - 4 \right].$$

Note Eq. 14.45.

14.11 Consider the grazing stream tube defined by Eq. 14.51. Show that the volume of fluid flow within this grazing tube per unit time is 2π times the value of the grazing stream function. (Note that the volume may be calculated on the plane, $\theta = \pi/2$. It is $\int(-U_\theta)2\pi r \mathrm{d}r$.)

14.12 Establish Eq. 14.53.

14.13 Potential flow around a cylinder transverse to the fluid flow is described in the vicinity of the cylinder by

$$\psi(\rho, \phi) = a_c U_\infty \left(\frac{\rho}{a_c} - \frac{a_c}{\rho}\right) \sin\phi$$

Discuss the threshold for inertia capture in this potential flow as described associated with a sphere at Eq. 14.62.

14.14 In certain types of heat exchangers, a gas flows normal to a bank of tubes carrying fluid at different temperature, and heat transfer occurs at the surface. Fouling of the outside surface of the tubes occurs as a result of particles depositing from the flow. If the tubes are 1 cm (outside diameter) and the gas velocity is 5 m/s, estimate the diameter of the largest particle (the density = 2 g/cm^3) that can be permitted in the gas stream without deposition on the tube. Assume that $\eta_g = 2.18 \cdot 10^{-4}$ g/cm s and $\rho_g = 6.61 \cdot 10^{-4}$ g/cm^3 for air at 100°C. For simplicity, consider that the air is already at the temperature of the fluid in the tubes. (Hint: see Eq. 14.63.)

14.15 Establish Eq. 14.70.

14.16 Rewrite Eq. 14.79 in terms of nondimensional variables, $u_\rho = U_\rho/U_\infty$, $u_\phi = U_\phi/U_\infty$, $\rho' = \rho/a_c$, and $Pe = 2a_c U_\infty/D$. If $Pe \gg 1$, the quantity in the bracket must be very large. Discuss that the term of the highest-degree derivative is the largest among the three in the bracket. Thus, when $Pe \gg 1$, the concentration boundary layer becomes noticeable.

14.17 Roughly estimate the thickness of the concentration boundary layer from Eqs. 14.79 and 14.80.

References

Adamczyk, Z. and Van de Ven, T.G.M., *J. Colloid Interface Sci. 84*, 497 (1981).

Bart, E., *Chem. Eng. Sci. 23*, 103 (1968).

Batchelor, G.K. and Green, J.T., *J. Fluid Mech. 56*, 375 (1972).

Bell, K.A., "Aerosol Deposition in Models of a Human Lung Bifurcation", Ph.D. thesis in chemical engineering, California Institute of Technology, (1974).

Blanchard, D.C., "From Raindrops to Volcanos: Adventures in Sea-Surface Meteorology", Doubleday, New York (1967).

Brenner, H., *Chem. Eng. Sci. 16*, 242 (1961).

Brock, J.R., *J. Colloid Interface Sci. 23*, 448 (1967).

Brun, R.J., Lewis, W., Perkins, P.J., and Serafini, J.S., NACA Report 1215 (1955).

Davis, C.N., "Aerosol Science", Academic Press, London (1966).

Davis, E.J. and Liao, S.C., *J. Colloid Interface Sci. 50*, 488 (1975).

Derjaguin, B.V., Storozhilova, A.I., and Rabinovich, Ya.I., *J. Colloid Interface Sci. 21*, 35 (1966).

Feke, D.L. and Schowalter, W.R., *J. Fluid Mech. 133*, 17 (1983).

Feke, D.L. and Schowalter, W.R., *J. Colloid Interface Sci. 106*, 203 (1986).

Friedlander, S.K., *J. Colloid Interface Sci. 23*, 157 (1967).
Fuchs, N.A., *Z. Phys. Chem. 171:34*, 199 (1934).
Goldman, A.J., Cox, R.G., and Brenner, H., *Chem. Eng. Sci. 22*, 637 (1967).
Goren, S.L., *J. Colloid Interface Sci. 44*, 356 (1973).
Greenfield, M.A., Koontz, R.L., and Houseknecht, D.F., *J. Colloid Interface Sci. 35*, 102 (1971).
Hampl, G.M., Kerker, M., Cooke, D., and Matijević, E., *J. Atmos. Sci. 28*, 1211 (1971).
Happel, J., *AIChE J. 5*, 174 (1959).
Happel, J. and Brenner, H., "Low Reynolds number hydrodynamics", Noordhoff International Publishing, Leyden, The Netherlands (1973).
Hidy, G.M. and Brock, J.R., *J. Coll. Sci. 20:6*, 477 (1965).
Hidy, G.M. and Brock, J.R., "The Dynamics of Aerocolloidal Systems, International Reviews in Aerosol Physics and Chemistry", Vol. 1, Pergamon Press, New York (1970).
Higashitani, K. and Matsuno, Y., *J. Chem. Eng. Japan 12*, 460 (1979).
Huser, R.B., "Coagulation of Knudsen Aerosols", Ph.D. thesis, University of Minnesota (1971).
Jacobson, S. and Brock, J.R., *J. Colloid Interface Sci.* 20, 544 (1965).
Jeans, J., "The Dynamical Theory of Gases", Dover, New York (1954).
Kirsch, A.A. and Stechkina, I.B., in "Fundamentals of Aerosol Science", ed. Shaw, D.T., John Wiley & Sons, New York (1978).
Kuwabara, S., *J. Phys. Soc. Japan 14*, 527 (1959).
Langmuir, I., *J. Am. Chem. Soc. 37*, 415 (1915).
Levich, V.G., "Physicochemical Hydrodynamics", Prentice Hall, New York (1962).
Lighthart, B. and Mohr, A.J., eds., "Atmospheric Microbial Aerosols", Chapman & Hall, New York, London (1994).
Mercer, T.T., in "Fundamentals of Aerosol Science", ed., Shaw, D.T., John Wiley, New York (1978).
Nelson, C.T., Baurmash, L., and Koontz, R.L., Proc. 9th AEC Air Cleaning Conference., Boston, MA, p. 860, Conf-660904 (1966).
Nicolaon, G., Kerker, M., Cooke, D.D., and Matijevic, E., *J. Colloid Interface Sci. 38*, 460 (1972).
Okuyama, K., Kousaka,Y., and Yoshida, T., *J. Chem. Eng. (Japan) 9*, 140 (1976).
Prieve, D.C. and Ruckenstein, E., *AIChE J. 20*, 1178 (1974).
Reichl, L.E., "A Modern Course in Statistical Mechanics", University of Texas Press, Austin (1980).
Rosenhead, L., "Laminar Boundary Layer", Oxford University Press (Clarendon), Oxford (1963), p. 171.
Russel, W.B., Saville, D.A., and Schowalter, W.R, "Colloidal Dispersions", Cambridge University Press, Cambridge New York (1989).
Smoluchowski, M., *Z. Phys. Chem. 92*, 129 (1917).
Spielman, L.A. and Cukor, P.M., *J. Colloid Interface Sci. 43*, 51 (1973).
Spielman, L.A. and Goren, S.L., *Environ. Sci. Technol. 2*, 279 (1968); *ibid. 4*, 135, (1970) with corrections in *ibid. 5*, 254 (1971).
Street, R.E., in "Rarified Gas Dynamics", ed., Devienne, F., Pergamon, New York (1960).
Suzuki, A., Ho, N.F.H., and Higuchi, A., *J. Colloid Interface Sci. 29*, 552 (1969).
Takamura, K., Goldsmith, H.L., and Mason, S.G., *J. Colloid Interface Sci. 82*, 175 (1981).
Twomey, S., "Atmospheric Aerosols", Elsevier Scientific Publishing Company, Amsterdam Oxford New York (1977), p. 161.
Van de Ven, T.G.M. and Mason, S.G., *J. Colloid Interface Sci. 57*, 505, 517 (1976); *Colloid Polym. Sci. 255*, 794 (1977).
Wagner, P.E., in "Aerosol Microphysics II", ed., Marlow, W.H., Springer-Verlag, Berlin Heidelberg New York (1982).
Wagner, P .E. and Pohl, F.G., *Gesellschaft Aerosolforsch. 6*, 147 (1978).
Wagner, P.E. and Pohl, F.G., *J. Aerosol Sci. 10*, 204 (1979).
Walter, H., *Aerosol Sci. 4*, 1 (1973).
Wong, J.B. and Johnstone, H.F., Collection of Aerosols by Fiber Mass, Tech. Report. 11, Eng. Expt., Station, University of Illinois (1953).
Woodcock, A.H., Kientzler, C.F., Arons, A.B., and Blanchard, D.C., *Nature 172*, 1144 (1953).
Yoshida, T., Okuyama, K., Kousaka, Y., and Kida, Y., *J. Chem. Eng. (Japan) 8*, 317 (1975).